Vibration Analysis of 2-PR(Pa)U- 2-PR(Pa)R New Parallel Mechanism

Mehran Mahboubkhah*
Department of Mechanical Engineering,
University of Tabriz, Iran
E-mail: Mahboobkhah@tabrizu.ac.ir
*Corresponding author

Sajjad Pakzad
Department of Mechanical Engineering,
University of Tabriz, Iran
E-mail: Pakzad@tabrizu.ac.ir

Morteza Homayoun Sadeghi
Department of Mechanical Engineering,
University of Tabriz, Iran
E-mail: morteza@tabrizu.ac.ir

Mir Mohammad Ettefagh
Department of Mechanical Engineering,
University of Tabriz, Iran
E-mail: ettefagh@tabrizu.ac.ir

Received: 28 October 2017, Revised: 7 December 2017, Accepted: 17 January 2018

Abstract: Parallel kinematic machines, are closed loop structures which have more accuracy, stiffness and ability to withstand high loads. In this paper the vibration equations of the new parallel mechanism, that has higher stiffness because of parallelogram system and fixed length pods, have been derived by analytical approach. Whereas the proposed mechanism is applied as a machine tools, its vibrational behavior investigation has key impact factor. All the kinematic chains of the mechanism have been taken into consideration to achieve the coupled system of equations. To extract mechanism natural frequencies, modal analysis is carried out using three methods including analytical, finite element (FEM) and experimental method on parallel mechanism which has four degrees of freedom including three linear motion along the x, y and z axes and a rotary motion about x axis. Finally the natural frequencies and mode shapes obtained from analytical, experimental and FEM were compared. It is worth noting that all the frequencies obtained from three methods had little differences.

Keywords: Modal test, Parallel mechanism, Vibration analysis

Reference: Mahboubkhah, M., Pakzad, S., Homayoun Sadeghi, M., and Ettefagh, M. M., "Vibration Analysis of 2-PR(Pa)U- 2-PR(Pa)R New Parallel Mechanism", Int J of Advanced Design and Manufacturing Technology, Vol. 11/No. 1, 2018, pp. 47-56.

Biographical notes: M. Mohboubkhah is associate professor in the Faculty of Mechanical Engineering, in University of Tabriz, Tabriz, Iran. His research interests include Machine Tools Design, Metrology and Robotics. **S. Pakzad** is PhD candidate in the Faculty of Mechanical Engineering, in University of Tabriz, Tabriz, Iran. **M. Homayoun Sadeghi** is Professor at the Department of Mechanical Engineering, in University of Tabriz, Tabriz, Iran. **M. M. Ettefagh** is associate professor in the mechanical engineering faculty of university of Tabriz.

1 INTRODUCTION

Parallel mechanisms are significantly used in many fields of engineering science and industries such as machining, metrology, flight simulator, simulated earthquake, medical equipment, and etc. In general, these mechanisms have two main bodies which are coupled with each other which act through multiple links in parallel mode [1]. In comparison to arms of traditional series, the potential benefits of parallel structures are as follows: higher kinematic accuracy, lighter weight and better structural rigidity, stable capacity and suitable position of saddle arrangement, low production cost and better load bearing ability, however, from application point of view limited workspace and technical complexity are two important disadvantages of parallel arms. Therefore the parallel kinematic machine are so suitable when the accuracy, rigidity, high speed and the ability to carry a heavy load is required in a limited workspace [2].

In terms of configuration and movement structure, parallel mechanisms are divided into two types of pods with fixed – length and variable – length: Mechanisms with fixed – length pods, in their own group and along the path of guides, are distinguishable. In these mechanism, the pods with fixed length are used which are connected to a saddle at their end part and the saddles are on motion through guides and this motion is carried out through a linear or rotational operators. In mechanisms with variable – length pods, rotational and spherical joints are fixed to fix and moving platforms by bolt and the only variable parameter is the pods length. The position and orientation of moving platform is determined by changing the pods length. In recent years, much research has been carried out on parallel robots. One of the evolutions which is already in industrial production, especially in the field of manufacturing, is the use of parallel mechanisms independently or as part of other industrial machinery.

Parallel robots with six degrees of freedom, generally suffers from small workspace, complex mechanical design, difficulty in making and controlling the move due to complicated kinematic analysis. To overcome these shortcomings, the new structures for parallel robots with fewer than six degrees of freedom are used. On the other hand, in many industrial cases, there is a need to provide facilities with more than three degrees of freedom with parallel arrangement as well as simpler arrangement compared to six degrees of freedom [3].

Vibration of machine tools directly influences the efficiency, accuracy and quality of machining surface and tool life. Thus, to predict dynamic behavior, machine tool vibration analysis is necessary and as a reason, it has become manufacturers and researchers interest [4]- [10]. Determining vibration characteristic of machine tools structure and knowing the dynamic behavior of structures, in addition to its usage in dynamics issues of the machining, is of special importance features in determination of suitable working conditions and selecting the appropriate machining parameters to avoid resonance areas in machining time.

To avoid chatter phenomenon in workshops, the operators choose the machining parameters cautiously. Moreover, in several cases, due to arising chatter, additional manually operations are needed to compensate defective surface finish of workpieces. In any case, reduction in efficiency is returning. In Renault automobile company, the excessive cost of machining of each cylinder block, due to arising chatter, is estimated to be 0.35€. For this company with three millions productions annually, chatter prevention is crucial [11]. In another study, Budak et al. [12] showed that, the machining time of a turbine blade decreases from 35 min to 19 min, when the machining operation is performed on the basis of predictive stability model.

Accurate computer simulation of machine tools structure and consideration of vibration behavior analysis using finite element software contribute to achieving natural frequencies and vibration mode shapes for machine tools construction; in this field, various research is carried out by researchers [13]- [17]. Considering vibration analysis of structures using finite element software plays an important role to provide correct plan to carry out precise experimental modal test .Since testing and modal analysis provide important information on the dynamic behavior of engineering structures as well as clever solving of vibration issues, it is used as an appropriate tool to study the dynamic behavior and to solve complex vibration issues on structural vibration of mechanical systems, especially machine tools.

From the application point of view, parallel mechanisms are divided in two major groups: first, mechanisms which are used as an interface in accurate vibration isolation and have little movement and second, mechanisms which are used for precise positioning. The vibration control of second groups even though having broad band, high power capability and appropriate sensors, is limited [18]. In order to machine work pieces accurately, in recent years, usage of these mechanisms as a table or spindle of machine tool, which requires precise, rigid and controllable components are dramatically increased. The used drivers in the positioning mechanisms inevitably have higher movement and a lower resolution; therefore, in the designed mechanisms for positioning, change in the mechanism configuration, displacement of moving platform or a change in mass and platform inertia and the applied load, probably will lead to alter the natural frequencies and vibration modes of mechanisms. Thus in the positioning mechanisms, regarding a wide range

of changes in the configuration of these mechanisms, prediction and prevention of the vibrations is possible. Mahboubkhah et al [19], [20] have examined free vibration of hexapod and its natural frequencies range for different configurations with two different methods, in one of the method, pod mass is neglected and equivalent stiffness of each pod is applied in vibration equations of the moving platform and in other method, the mass of the pod is applied in the calculation of free vibration of the mechanism.

In these two studies, the results of the mathematical model with the results of finite element are studied comparatively. A similar consideration is carried out by Pedrammehr and his colleagues for forced vibration of hexapod machine tool's table [21], [22]. Law et al [23] have modeled a parallel–series hybrid mechanism and have used it to consider the dependency of the mechanism dynamic behavior to the position. Based on their own model, they also have experimentally validated mechanism position dependency. Other areas related to vibrations of parallel mechanisms could be found in [24]- [28] references.

In this paper, in order to determine the natural frequencies and vibration mode shapes, a parallel mechanism with 4 degrees of freedom (Dof) is considered using three methods of theoretical, FEM and experimental method. For this purpose the vibration model of a parallel mechanism has been presented and the relevant explicit equations have been derived. In this model, mass, inertia, stiffness and damping of various elements comprising the mechanism have been taken into consideration. Then the eigenvalue problem has been solved for the moving platform as the end effector. These theoretical results have been compared with the results of FEM (Ansys) simulation. Then experimental modal test was conducted to evaluate the accuracy of the results. Finally, Comparing the results, showed satisfactory of the results of theoretical, FEM and experimental modal analysis, this comparison is based on natural frequencies and mode shapes obtained from methods.

2 VIBRATION MODEL OF THE MECHANISM

A schematic view of the mechanism can be observed in Fig. 1. Parallel mechanism of this robot provides 4 degrees of freedom which includes the displacement in x, y and z axis and rotation about x axis. The fourth degree of freedom (rotational motion) leads to increased maneuverability as well as its usefulness compared to that of mechanisms with three degrees of freedom. This mechanism is interconnected by two types of fraternal chain 2-PR (Pa) U-2-PR (Pa) R, two chains of PR (Pa) R and two chains of PR (Pa) U in which P, R, Pa and U represent sliding joint, hinge joint, and parallelogram or universal joint respectively. Two coordinate systems are used in order to define the motion of the mechanism. The global coordinate system, {O}, is fixed at the center of the stationary platform. The local coordinate system, {P}, is fixed to the geometry center of the platform and moves and rotates with it. The vector $\boldsymbol{P} = (x_0 \quad y_0 \quad z_0)$ defined in {O} specifies the position of frame {P}. The orientation of frame {P} and thus the platform is described by (θ_x). This rotation can be expressed in frame {W} with the aid of a rotation matrix, $\boldsymbol{R_P}$ (Appendix a).

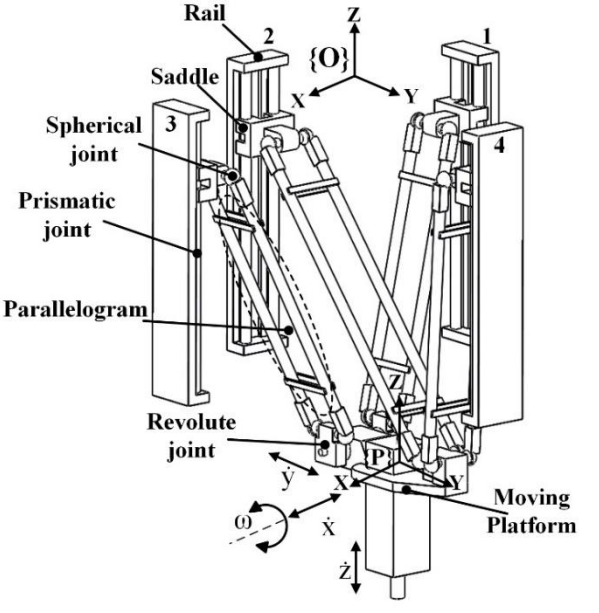

Fig. 1 2-PR(Pa)U-2-PR(Pa)R parallel mechanism with 4 degrees of freedom

A flexible model has been proposed by the authors for deriving the vibration equations of the presented mechanism. In this model, pods, the upper and lower joints and the saddles have been considered as flexible elements. The platform carrying the spindle and frame of mechanism during machining operations should be sufficiently stiff in order to resist undesirable deformations ensuing from the machining loads. These parts can, therefore, be considered rigid with negligible damping. It is assumed that the joints are well lubricated and can be considered frictionless with negligible rotational damping. It is noteworthy that the instantaneous position and orientation of the platform have profound impact on the stiffness and dynamic behavior of the mechanism and should be taken into consideration. The flexible model of the mechanism is shown in Fig. 2. In this figure, only one pod is depicted. The parameters shown in this figure are as follows: $\boldsymbol{M}_P$ and $\boldsymbol{I}_P$ are the total mass and mass inertia matrices of the moving platform together with the spindle, $\boldsymbol{M}_L$ and $\boldsymbol{M}_S$ are the mass of pods and saddles respectively (i=1-4 for

four pods); l_{Pi}, l_{Li} and l_{Si} are the displacements of the platform, pods and saddles along pod's longitudinal axis, respectively. K_{lJi}, K_{Li}, K_{uJi} and $K_{Si}$are the stiffness coefficients of the lower joints, pods, upper joints, and saddles, respectively. C_{lJi} ,C_{Li}, C_{uJi} and $C_{Si}$are the damping coefficients. Δl_{lLi} is the total deflection from the lower joint up to the mass center of pod along the latter's longitudinal axis; Δl_{uLi} is the longitudinal deflection between the mass centers of the pod and saddle of the i^{th} pod; and Δl_{Si} is the deflection of the saddle along the axis of the i^{th} pod up to the surface of the foundation.

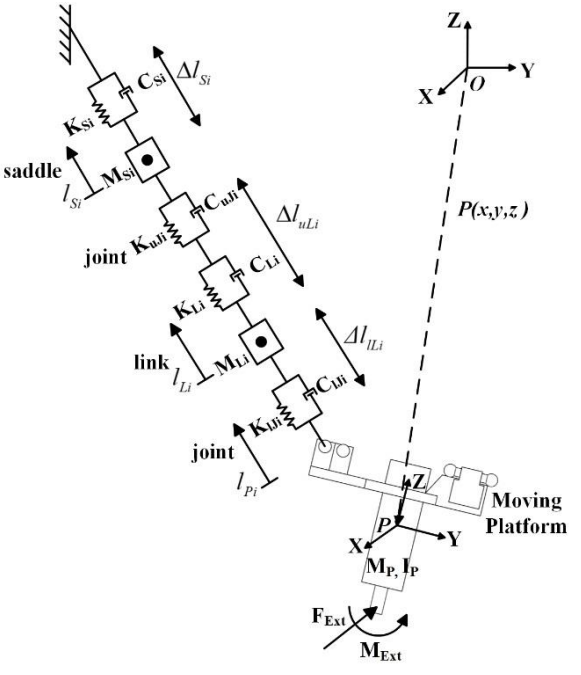

Fig. 2 Vibration model of the mechanism

3 VIBRATION EQUATION OF THE MECHANISM

Free body diagrams of various structural elements of the mechanism is illustrated in Fig. 3. In this figure, $\ddot{\boldsymbol{X}}_{\boldsymbol{P}}$ and $\ddot{\boldsymbol{\theta}}_{\boldsymbol{P}}$ are the linear and angular accelerations of the platform's center corresponding to $\ddot{l}_P$ defined in {O}, respectively, $\ddot{l}_P$, $\ddot{l}_L$ and $\ddot{l}_S$ are accelerations of the moving platform, pods and saddles along i^{th} pod, respectively; and $\boldsymbol{F_{Ext}}$ and $\boldsymbol{M_{Ext}}$ are harmonic machining force and moment applied on the moving platform and expressed in {P}. F_{KSi} and F_{CSi} are the spring and damping forces of the saddle and can be expressed as follows:

$$F_{KSi} = K_{Si} \cdot \Delta l_{Si} \ , \ F_{CSi} = C_{Si} \cdot \dot{\Delta} l_{Si} \tag{1}$$

Where $\dot{\Delta} l_{Si}$, is the total variation of the velocity of the saddle.

F_{KuLi} and F_{CuLi} are the spring and damping forces of the upper joint and pods and calculated as follows:

$$F_{KuLi} = K_{uLi} \cdot \Delta l_{uLi} \ , \ F_{CuLi} = C_{uLi} \cdot \dot{\Delta} l_{uLi} \tag{2}$$

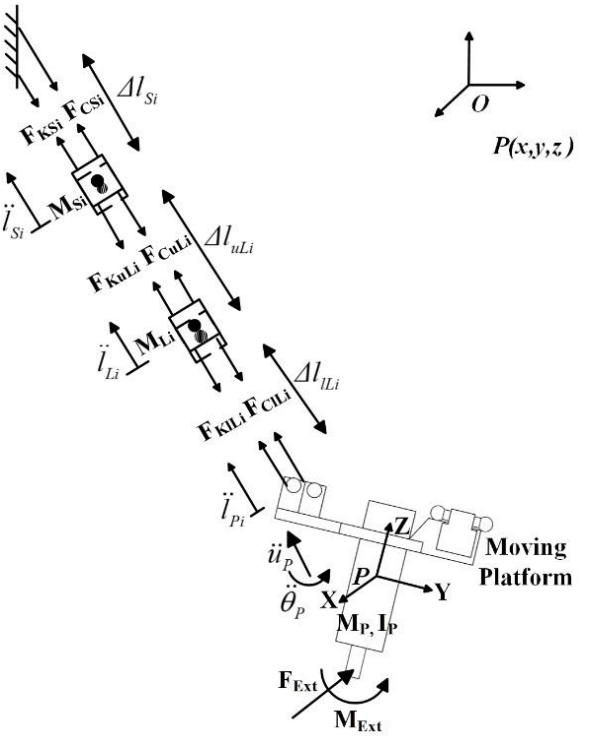

Fig. 3 Free body diagrams of the mechanism's structural units

$\dot{\Delta} l_{uLi}$ is the velocity variation of the upper joint and pods. K_{uLi} and C_{uLi} are estimated as follows:

$$\begin{aligned} 1/K_{uLi} &= 1/K_{uJi} + 1/K_{Li} \\ 1/C_{uLi} &= 1/C_{uJi} + 1/C_{Li} \end{aligned} \tag{3}$$

F_{KlLi} and F_{ClLi} are the spring and damping forces of the lower joint and estimated as follows:

$$F_{KlLi} = K_{lLi} \cdot \Delta l_{lLi} \ , \ F_{ClLi} = C_{lLi} \cdot \dot{\Delta} l_{lLi} \tag{4}$$

$\dot{\Delta} l_{lLi}$ is the total variation of the velocity of lower joint. Newtonian vibration equation for the lumped mass of the platform can be written as follows:

$$M_P \ddot{\boldsymbol{u}}_{\boldsymbol{P}} + \sum \boldsymbol{l_{io}} F_{ClLi} + \sum \boldsymbol{l_{io}} F_{KlLi} = \boldsymbol{R_P F_{Ext}} \tag{5}$$

Where $\boldsymbol{l_{io}}$ is the unit vector along i^{th} pod. The moment (Euler) vibration equation of the platform can be expressed as follows:

$$\begin{aligned} &\boldsymbol{R_P}(\boldsymbol{M_{Ext}} + \boldsymbol{r_T} \times \boldsymbol{F_{Ext}}) - \sum \boldsymbol{R_P} \cdot {}^{\boldsymbol{P}}\boldsymbol{b_i} \times \\ &\boldsymbol{l_{io}} F_{ClLi} + \sum \boldsymbol{R_P} \cdot {}^{\boldsymbol{P}}\boldsymbol{b_i} \times \boldsymbol{l_{io}} F_{KlLi} = \boldsymbol{I_P} \ddot{\boldsymbol{\theta}}_{\boldsymbol{P}} \end{aligned} \tag{6}$$

Where $^{P}\boldsymbol{b_i}$, is the position vector of i^{th} joint expressed in {P}. Using following definition:

$$\boldsymbol{b_i} = \boldsymbol{R_P} \cdot {}^{P}\boldsymbol{b_i} \tag{7}$$

Eq. 6 can be expressed as follows:

$$\begin{aligned}&\boldsymbol{I_P}\ddot{\boldsymbol{\theta}}_{\boldsymbol{P}} + \sum \boldsymbol{b_i} \times \boldsymbol{l_{io}} F_{ClLi} + \sum \boldsymbol{b_i} \times \\ &\boldsymbol{l_{io}} F_{KlLi} = \boldsymbol{R_P}(\boldsymbol{M_{Ext}} + \boldsymbol{r_T} \times \boldsymbol{F_{Ext}})\end{aligned} \tag{8}$$

Where $\boldsymbol{r_T}$ is a vector indicating the position of the external forces relative to the platform's gravity center. Coupling Eqs. 5 and 8 yields:

$$\begin{aligned}&\begin{bmatrix} M_P \boldsymbol{I_{3\times3}} & \boldsymbol{0} \\ \boldsymbol{0} & \boldsymbol{I_P} \end{bmatrix} \begin{Bmatrix} \ddot{\boldsymbol{X}}_{\boldsymbol{P}} \\ \ddot{\boldsymbol{\theta}}_{\boldsymbol{P}} \end{Bmatrix} + \boldsymbol{J_x^T} \boldsymbol{C_{lL}} \cdot \dot{\Delta}\boldsymbol{l_{lL}} + \\ &\boldsymbol{J_x^T} \boldsymbol{K_{lL}} \cdot \Delta \boldsymbol{l_{lL}} = \begin{bmatrix} \boldsymbol{R_P} \boldsymbol{F_{Ext}} \\ \boldsymbol{R_P}(\boldsymbol{M_{Ext}} + \boldsymbol{r_T} \times \boldsymbol{F_{Ext}}) \end{bmatrix}\end{aligned} \tag{9}$$

Where $\boldsymbol{J_x^T}$ is the transpose of the Jacobian matrix (Appendix a), $\boldsymbol{K_{lL}}$and $\boldsymbol{C_{lL}}$, 4×4 diagonal matrices, the diagonal elements of which are the stiffness and damping coefficients of the lower joints, respectively, and $\boldsymbol{I_{3\times3}}$ is a 3×3 identity matrix. The machining load is denoted here by $\boldsymbol{F^V}$ which can be written as follows:

$$\boldsymbol{F^V} = \begin{bmatrix} \boldsymbol{R_P} \boldsymbol{F_{Ext}} \\ \boldsymbol{R_P}(\boldsymbol{M_{Ext}} + \boldsymbol{r_T} \times \boldsymbol{F_{Ext}}) \end{bmatrix} \tag{10}$$

If $\boldsymbol{X_P}$ and $\boldsymbol{\theta_P}$ denote small linear and rotational displacements of the platform's center corresponding to $\Delta\boldsymbol{l_{lL}}$; and $\dot{\boldsymbol{X}}_{\boldsymbol{P}}$ and $\dot{\boldsymbol{\theta}}_{\boldsymbol{P}}$ are variations of linear and rotational speeds of the platform's center corresponding to $\dot{\Delta}\boldsymbol{l_{lL}}$ expressed in Cartesian coordinates, then:

$$\Delta \boldsymbol{l_{lL}} = \boldsymbol{J_x} \begin{Bmatrix} \boldsymbol{X_P} \\ \boldsymbol{\theta_P} \end{Bmatrix} \;,\; \dot{\Delta}\boldsymbol{l_{lL}} = \boldsymbol{J_x} \begin{Bmatrix} \dot{\boldsymbol{X}}_{\boldsymbol{P}} \\ \dot{\boldsymbol{\theta}}_{\boldsymbol{P}} \end{Bmatrix} \tag{11}$$

Substituting Eqs. 10 and 11 in Eq. 9 yields:

$$\begin{aligned}&\begin{bmatrix} M_P \boldsymbol{I_{3\times3}} & \boldsymbol{0} \\ \boldsymbol{0} & \boldsymbol{I_P} \end{bmatrix} \begin{Bmatrix} \ddot{\boldsymbol{X}}_{\boldsymbol{P}} \\ \ddot{\boldsymbol{\theta}}_{\boldsymbol{P}} \end{Bmatrix} + \boldsymbol{J_x^T} \boldsymbol{C_{lL}} \boldsymbol{J_x} \begin{Bmatrix} \dot{\boldsymbol{X}}_{\boldsymbol{P}} \\ \dot{\boldsymbol{\theta}}_{\boldsymbol{P}} \end{Bmatrix} + \\ &\boldsymbol{J_x^T} \boldsymbol{K_{lL}} \boldsymbol{J_x} \begin{Bmatrix} \boldsymbol{X_P} \\ \boldsymbol{\theta_P} \end{Bmatrix} = \boldsymbol{F^V}\end{aligned} \tag{12}$$

Vibration equation for the lumped mass of the pod is obtained as follows:

$$\begin{aligned}&M_{Li}\ddot{l}_{Li} - F_{KlLi} - F_{ClLi} + F_{KuLi} + F_{CuLi} = \\ &0\end{aligned} \tag{13}$$

Substituting the spring and damping forces from Eqs. 2 and 4:

$$\begin{aligned}&M_{Li}\ddot{l}_{Li} - K_{lLi} \cdot \Delta l_{lLi} - C_{lLi} \cdot \dot{\Delta} l_{lLi} + K_{uLi} \cdot \\ &\Delta l_{uLi} + C_{uLi} \cdot \dot{\Delta} l_{uLi} = 0\end{aligned} \tag{14}$$

Considering similar definition as those expressed for the platform in Eq. 12:

$$\begin{aligned}&\boldsymbol{M_L} \boldsymbol{J_x} \begin{Bmatrix} \ddot{\boldsymbol{X}}_{\boldsymbol{L}} \\ \ddot{\boldsymbol{\theta}}_{\boldsymbol{L}} \end{Bmatrix} - \boldsymbol{K_{lL}} \boldsymbol{J_x} \begin{Bmatrix} \boldsymbol{X_P} \\ \boldsymbol{\theta_P} \end{Bmatrix} - \\ &\boldsymbol{C_{lL}} \boldsymbol{J_x} \begin{Bmatrix} \dot{\boldsymbol{X}}_{\boldsymbol{P}} \\ \dot{\boldsymbol{\theta}}_{\boldsymbol{P}} \end{Bmatrix} + \boldsymbol{K_{uL}} \boldsymbol{J_x} \begin{Bmatrix} \boldsymbol{X_L} \\ \boldsymbol{\theta_L} \end{Bmatrix} + \\ &\boldsymbol{C_{uL}} \boldsymbol{J_x} \begin{Bmatrix} \dot{\boldsymbol{X}}_{\boldsymbol{L}} \\ \dot{\boldsymbol{\theta}}_{\boldsymbol{L}} \end{Bmatrix} = 0\end{aligned} \tag{15}$$

Where $\boldsymbol{M_L}$ is a 4×4 diagonal matrix, the elements of which represent the masses of the four pods; $\boldsymbol{X_L}$ and $\boldsymbol{\theta_L}$ are small linear and rotational displacements of the platform's center corresponding to $\Delta\boldsymbol{l_{uL}}$, and $\dot{\boldsymbol{X}}_{\boldsymbol{L}}$ and $\dot{\boldsymbol{\theta}}_{\boldsymbol{L}}$ are variations of linear and rotational speeds of the platform's center corresponding to $\dot{\Delta}l_{uL}$ expressed in Cartesian coordinates. Multiplying both sides of Eq. 17 by $\boldsymbol{J_x^{-1}}$:

$$\begin{aligned}&\boldsymbol{M_L} \begin{Bmatrix} \ddot{\boldsymbol{X}}_{\boldsymbol{L}} \\ \ddot{\boldsymbol{\theta}}_{\boldsymbol{L}} \end{Bmatrix} - \boldsymbol{K_{lL}} \begin{Bmatrix} \boldsymbol{X_P} \\ \boldsymbol{\theta_P} \end{Bmatrix} - \boldsymbol{C_{lL}} \begin{Bmatrix} \dot{\boldsymbol{X}}_{\boldsymbol{P}} \\ \dot{\boldsymbol{\theta}}_{\boldsymbol{P}} \end{Bmatrix} + \\ &\boldsymbol{K_{uL}} \begin{Bmatrix} \boldsymbol{X_L} \\ \boldsymbol{\theta_L} \end{Bmatrix} + \boldsymbol{C_{uL}} \begin{Bmatrix} \dot{\boldsymbol{X}}_{\boldsymbol{L}} \\ \dot{\boldsymbol{\theta}}_{\boldsymbol{L}} \end{Bmatrix} = 0\end{aligned} \tag{16}$$

Vibration equation for the lumped mass of the saddles can be expressed as follows:

$$M_{Si}\ddot{l}_{Si} + F_{KSi} + F_{CSi} - F_{KuLi} - F_{CuLi} = 0 \tag{17}$$

Similar manipulations as those performed for Eq. 16 yield:

$$\begin{aligned}&\boldsymbol{M_S} \begin{Bmatrix} \ddot{\boldsymbol{X}}_{\boldsymbol{S}} \\ \ddot{\boldsymbol{\theta}}_{\boldsymbol{S}} \end{Bmatrix} + \boldsymbol{K_S} \begin{Bmatrix} \boldsymbol{X_S} \\ \boldsymbol{\theta_S} \end{Bmatrix} + \boldsymbol{C_S} \begin{Bmatrix} \dot{\boldsymbol{X}}_{\boldsymbol{S}} \\ \dot{\boldsymbol{\theta}}_{\boldsymbol{S}} \end{Bmatrix} - \\ &\boldsymbol{K_{uL}} \begin{Bmatrix} \boldsymbol{X_L} \\ \boldsymbol{\theta_L} \end{Bmatrix} - \boldsymbol{C_{uL}} \begin{Bmatrix} \dot{\boldsymbol{X}}_{\boldsymbol{L}} \\ \dot{\boldsymbol{\theta}}_{\boldsymbol{L}} \end{Bmatrix} = 0\end{aligned} \tag{18}$$

Where $\boldsymbol{M_S}$ is a 4×4 diagonal matrix the elements of which represent the masses of the four saddles; $\boldsymbol{X_S}$ and $\boldsymbol{\theta_S}$, small linear and rotational displacements of the platform's center corresponding to Δl_S, and $\dot{\boldsymbol{X}}_{\boldsymbol{S}}$ and $\dot{\boldsymbol{\theta}}_{\boldsymbol{S}}$, variations of linear and rotational speeds of the platform's center corresponding to $\dot{\Delta}l_S$ expressed in Cartesian coordinates. Coupling Eqs. 12, 16 and 18 yields a system of vibration equations consisting of 12×12 matrices, as follows:

$$\begin{aligned}&\boldsymbol{M_V}[\ddot{\boldsymbol{X}}_{\boldsymbol{P}} \quad \ddot{\boldsymbol{\theta}}_{\boldsymbol{P}} \quad \ddot{\boldsymbol{X}}_{\boldsymbol{L}} \quad \ddot{\boldsymbol{\theta}}_{\boldsymbol{L}} \quad \ddot{\boldsymbol{X}}_{\boldsymbol{S}} \quad \ddot{\boldsymbol{\theta}}_{\boldsymbol{S}}]^{\boldsymbol{T}} + \\ &\boldsymbol{C_V}[\dot{\boldsymbol{X}}_{\boldsymbol{P}} \quad \dot{\boldsymbol{\theta}}_{\boldsymbol{P}} \quad \dot{\boldsymbol{X}}_{\boldsymbol{L}} \quad \dot{\boldsymbol{\theta}}_{\boldsymbol{L}} \quad \dot{\boldsymbol{X}}_{\boldsymbol{S}} \quad \dot{\boldsymbol{\theta}}_{\boldsymbol{S}}]^{\boldsymbol{T}} + \\ &\boldsymbol{K_V}[\boldsymbol{X_P} \quad \boldsymbol{\theta_P} \quad \boldsymbol{X_L} \quad \boldsymbol{\theta_L} \quad \boldsymbol{X_S} \quad \boldsymbol{\theta_S}]^{\boldsymbol{T}} = \\ &[\boldsymbol{F^V} \quad \boldsymbol{0} \quad \boldsymbol{0}]^{\boldsymbol{T}}\end{aligned} \tag{19}$$

Where $\boldsymbol{M_V}$, $\boldsymbol{C_V}$ and $\boldsymbol{K_V}$ are, respectively, the mass, damping and stiffness matrices of the mechanism structure. The total mass matrix, $\boldsymbol{M_V}$, is obtained by coupling individual mass and inertia matrices, as follows:

$$\boldsymbol{M_V} = \begin{bmatrix} \begin{bmatrix} M_P\boldsymbol{I_{3\times3}} & \boldsymbol{0_{3\times1}} \\ \boldsymbol{0_{1\times3}} & \boldsymbol{I_P} \end{bmatrix} & \boldsymbol{0_{4\times4}} & \boldsymbol{0_{4\times4}} \\ \boldsymbol{0_{4\times4}} & \boldsymbol{M_L} & \boldsymbol{0_{4\times4}} \\ \boldsymbol{0_{4\times4}} & \boldsymbol{0_{4\times4}} & \boldsymbol{M_S} \end{bmatrix} \quad (20)$$

The total damping matrix, $\boldsymbol{C_V}$, is also obtained by coupling individual damping matrices, as follows:

$$\boldsymbol{C_V} = \begin{bmatrix} \boldsymbol{J_x^T C_{lL} J_x} & \boldsymbol{-J_x^T C_{lL} J_x} & \boldsymbol{0_{4\times4}} \\ \boldsymbol{-C_{lL}} & \boldsymbol{C_{uL} + C_{lL}} & \boldsymbol{-C_{uL}} \\ \boldsymbol{0_{4\times4}} & \boldsymbol{-C_{uL}} & \boldsymbol{C_S + C_{uL}} \end{bmatrix} \quad (21)$$

Where $\boldsymbol{C_{lL}}$, $\boldsymbol{C_{uL}}$ and $\boldsymbol{C_S}$ are 4×4 diagonal matrices the elements of which represent the damping coefficients of lower joints, pods and upper joints, and saddles.
The total stiffness matrix, $\boldsymbol{K_V}$, is obtained, similarly, as follows:

$$\boldsymbol{K_V} = \begin{bmatrix} \boldsymbol{J_x^T K_{lL} J_x} & \boldsymbol{-J_x^T K_{lL} J_x} & \boldsymbol{0_{4\times4}} \\ \boldsymbol{-K_{lL}} & \boldsymbol{K_{uL} + K_{lL}} & \boldsymbol{-K_{uL}} \\ \boldsymbol{0_{4\times4}} & \boldsymbol{-K_{uL}} & \boldsymbol{K_S + K_{uL}} \end{bmatrix} \quad (22)$$

Where $\boldsymbol{K_{lL}}$, $\boldsymbol{K_{uL}}$ and $\boldsymbol{K_S}$ are 4×4 diagonal matrices the elements of which represent the stiffness coefficients of lower joints, pods and upper joints, and saddles. The vibration of the mechanism structure can, ultimately, be analyzed by Eq. 19 when its matrix coefficients are specified.

4 NATURAL FREQUENCIES OF THE MECHANISM

In order to obtain the natural frequencies of the mechanism, the external loads and the damping term are dropped from Eq. 19 giving the following characteristic equation for the mechanism:

$$\boldsymbol{M_V}[\ddot{\boldsymbol{X}}_{\boldsymbol{P}} \quad \ddot{\boldsymbol{\theta}}_{\boldsymbol{P}} \quad \ddot{\boldsymbol{X}}_{\boldsymbol{L}} \quad \ddot{\boldsymbol{\theta}}_{\boldsymbol{L}} \quad \ddot{\boldsymbol{X}}_{\boldsymbol{S}} \quad \ddot{\boldsymbol{\theta}}_{\boldsymbol{S}}]^T + \boldsymbol{K_V}[\boldsymbol{X_P} \quad \boldsymbol{\theta_P} \quad \boldsymbol{X_L} \quad \boldsymbol{\theta_L} \quad \boldsymbol{X_S} \quad \boldsymbol{\theta_S}]^T = \boldsymbol{0} \quad (23)$$

The natural frequencies of investigated structure regarding to Eq. 23 could be obtained by a code written in MATLAB environment. Another methods also, has been represented to verify the results of the constructed equations.

5 STRUCTURAL MODELING AND MODAL ANALYSIS BY FEM

Structural modeling was carried out according to its actual dimensions in Solid Works software. To achieve accurate simulation results, it is attempted to consider design details, precise measurements while modeling. Then to apply analysis, the presented model was inserted to finite element ANSYS workbench and the essential information, according to Table 1, such as material properties, boundary and contact conditions, type of elements and modal analysis method are defined. Type of mechanism meshing is depicted in Fig. 4.

Table 1 The defined properties in ANSYS software

Material	Aluminum Alloy
Density	2770 kg/m^3
Poisson's Ratio	0.33
Young's Modulus	71 GPa
Element type	SOLID 187, SOLID 186, CONTA174, CONTA175, TARGE170, COMBIN14
Number of Elements	10721
Number of Nodes	20162
Analysis type	Direct
Frequency type	0-1000 Hz

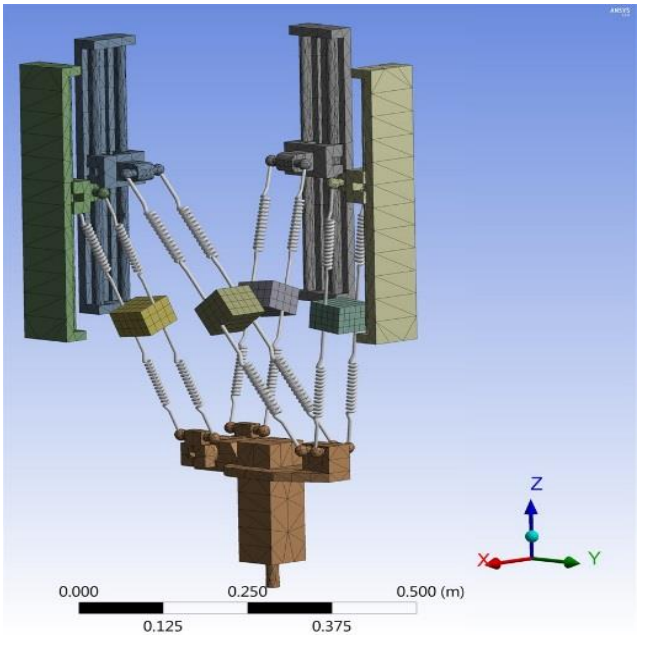

Fig. 4 The discretized model of parallel mechanism

6 EXPERIMENTAL MODAL ANALYSIS

The experimental modal analysis is performed on real sample structure to analyze dynamic behavior of the system. In modal test the exerted force by the exciter and structure response are measured simultaneously. Experimental modal test is performed with roving accelerometer method using the equipment presented in Table 2, in this method, the force is applied at a certain point of structure and the response is taken by the accelerometer in different points of the structure (Fig. 5). By keeping the force in moving platform of the mechanism and getting the response in 26 different points of the moving platform, pods and rails as shown in Fig. 6, the modal test is carried out. Moreover, the force is applied only in one point, in X direction on the moving platform and the response is taken in X, Y and Z directions for each 26 points and corresponding responses are obtained for different points and directions. The results of the tests, using the PULSE Labshop software as a frequency response function (FRF) are obtained for different parts. In order to extract the natural frequencies and mode shapes related to the experimental modal test, the studied parallel mechanism structure is modeled in ME'scope software. Then the FRF for each test point is transmitted to the software.

Table 2 Equipment of experimental modal analysis

Multi Analyzer System	B&K 3560
Shaker	B&K 4890
Accelerometer	B&K 4507
Force Sensor	B&K 8201

Fig. 5 Modal test of parallel mechanism

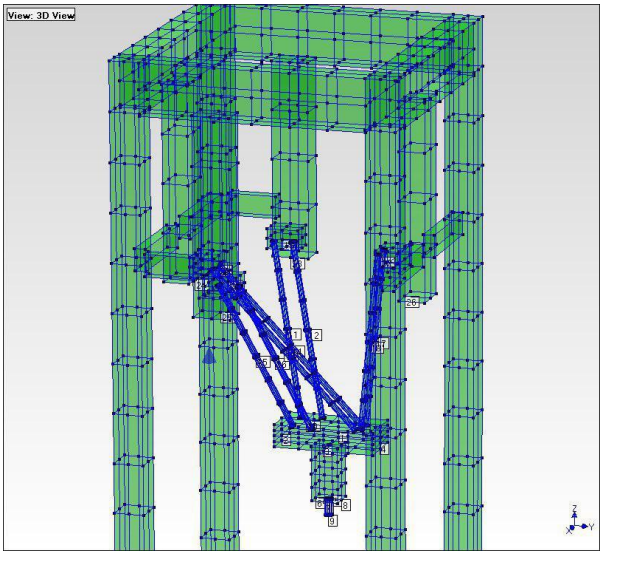

Fig. 6 Modal analysis model and points in ME'scope

7 RESULTS

Using Eq. 23 and by the aid of programs developed in MATLAB, The natural frequencies of the moving platform are estimated and given in Table 3. In order to verify the results, the natural frequencies of the mechanism for defined position (Appendix b) have also been obtained by FEM modal analysis.

A distinguishing feature of the mechanism that can be inferred from the mode shapes is the distinct vibration modes, irrespective of few exceptions. Linear vibration along x, y and z axes prevails in the first, second and third modes. The forth mode are rotational, around x axis.

Therefore, modal analysis performed experimental method in frequency range of zero to 1000 Hz, then 4 first natural frequencies of the machine tool are obtained. In Fig. 7 comparison of the analytical, FEM and experimental results are illustrated. FEM simulation for the mode shapes of vibration are illustrated in Figs. 8-11, respectively.

Table 3 Natural frequencies obtained by analytical approach

Mode No.	Natural frequency (Hz)
1	102.42
2	119.59
3	384.02
4	522.95

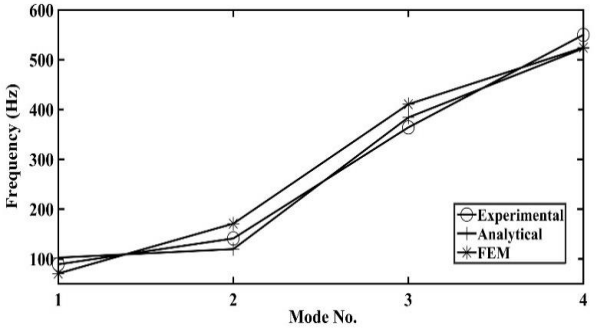

Fig. 7 Comparison of the analytical, FEM and experimental results

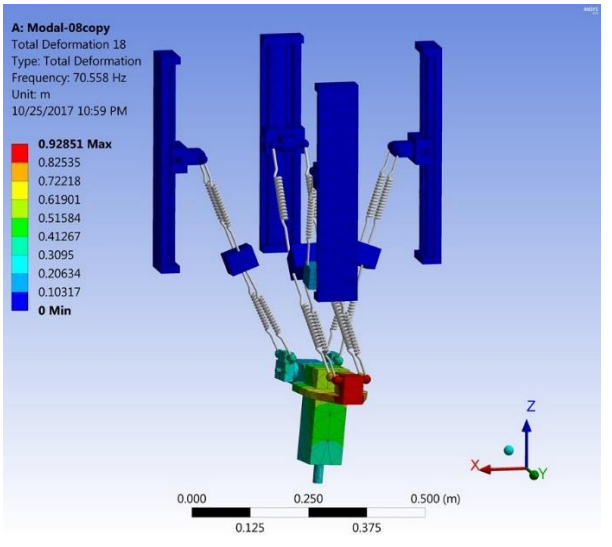

Fig. 8 First mode shapes of vibration in X direction

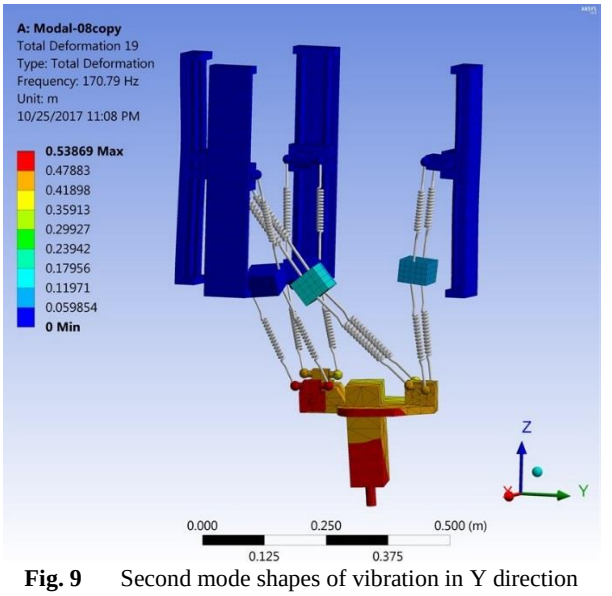

Fig. 9 Second mode shapes of vibration in Y direction

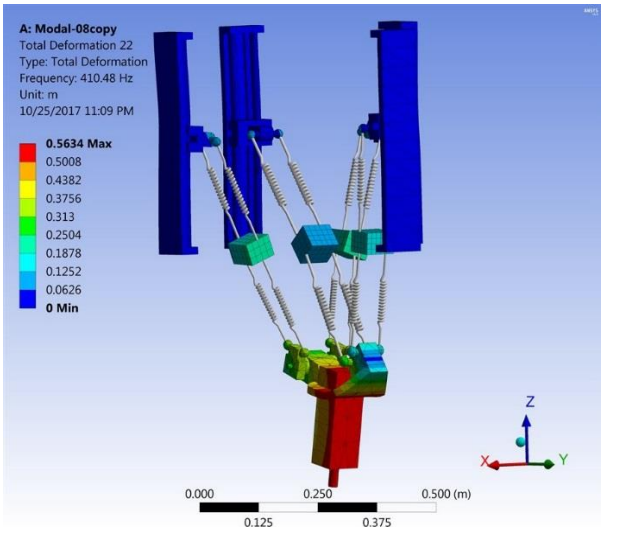

Fig. 10 Third mode shapes of vibration in Z direction

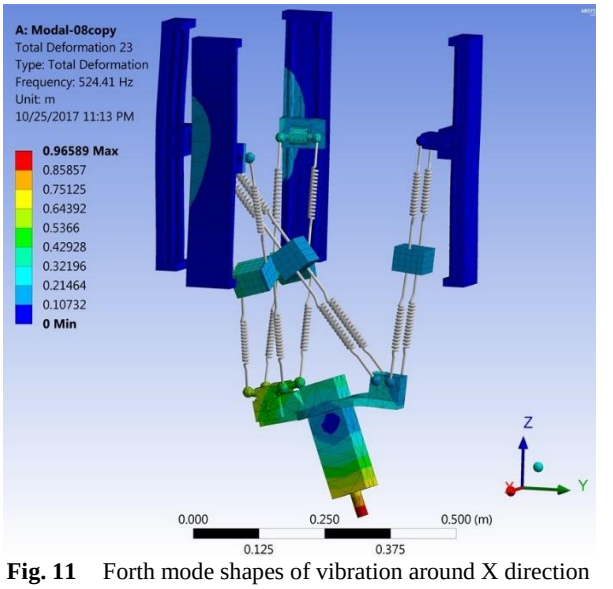

Fig. 11 Forth mode shapes of vibration around X direction

8 CONCLUSION

In this paper a parallel mechanism machine tool with 4Dof was modeled and analyzed by three methods. The vibration equations of the parallel mechanism have been derived by analytical approaches. All the kinematic chains of the mechanism have been taken into consideration to achieve the coupled system of equations. Natural frequencies and mode shapes of the structure were extracted through FEM modal analysis. Moreover, experimental modal test was carried out on structure of mechanism and its vibrational characteristics were obtained.

A distinguishing feature of the mechanism is its distinct vibration modes. Linear vibration in horizontal plane prevails in the first and second modes. The third modes are mainly occurs vertically. The forth mode of vibration mainly occurs around X axis. The linear vibration of the moving table occurs in lower modes with frequencies changing in the range of 102 to 384 Hz. The frequencies of rotational or coupled modes of vibration are in 522 Hz. It is obvious that more frequencies appear in practice as the mechanism elements are actually continuous masses.

Finally, the natural frequencies and mode shapes obtained from analytical, experimental and FEM methods were compared. It is worth noting that all the frequencies obtained from analytical, experimental and FEM methods had little differences.

9 APPENDIX

a)

The rotation matrix is obtained as follows:

$$\boldsymbol{R_p} = \begin{bmatrix} 1 & 0 & 0 \\ 0 & cos\,\theta & sin\,\theta \\ 0 & -sin\,\theta & cos\,\theta \end{bmatrix} \tag{A1}$$

The inverse Jacobian matrix can be expressed as:

$$\boldsymbol{J_x} = \begin{bmatrix} \mathrm{l}_1^{\mathrm{T}} & (\mathrm{b}_1 \times \mathrm{l}_1) \cdot \hat{\mathrm{i}} \\ \vdots & \vdots \\ \mathrm{l}_4^{\mathrm{T}} & (\mathrm{b}_4 \times \mathrm{l}_4) \cdot \hat{\mathrm{i}} \end{bmatrix} \tag{A2}$$

b) Mechanism Specifications:

Figure A1 depicts a schematic diagram of the kinematic parameters of the manipulator. The origin of global coordinate frame,$\{\boldsymbol{O}\}$, is placed at the beginning of each prismatic joint's rail via vector $\boldsymbol{a_i}$ and the position of the i^{th} prismatic joint from the base point of the rail is displayed by vector $\boldsymbol{d_i}$.

The vector $\boldsymbol{l_i}$ is in same direction and equal in magnitude to the links' lengths of the i^{th} arm and, as shown in Fig. A1, $\boldsymbol{c_i}$ is the vector attached to the i^{th} connector beginning from the midpoint of the spherical joints and ending at the revolute axis of the connector. It should be noted that for $\boldsymbol{i = 2,4}$, since there is no connector, then $\boldsymbol{c_i = 0}$.

Furthermore, $\boldsymbol{b_i}$ is a vector attached to the moving platform which connects the origin of the platform coordinate frame, $\{\boldsymbol{P}\}$, to the end of i^{th} parallelograms. Geometric and inertia properties of the manipulator under study are mentioned in Table A1.

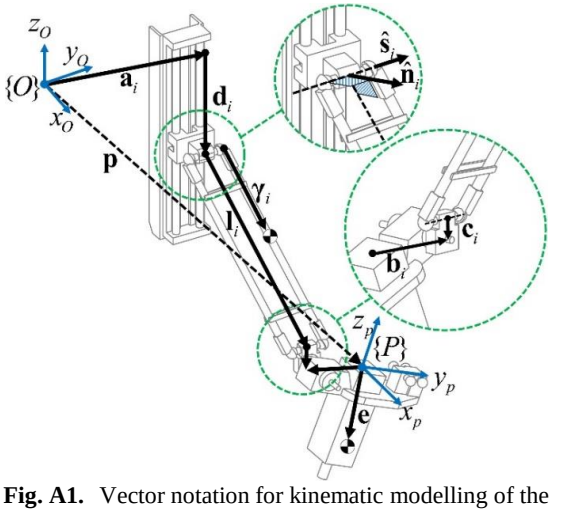

Fig. A1. Vector notation for kinematic modelling of the manipulator under study

Table A1 Geometric and inertia properties of mechanism

Parameter		Value
$\boldsymbol{l_i}$	$i = 1,3,4$	461 [mm]
	$i = 2$	561 [mm]
$\boldsymbol{c_i}$	$i = 1,3$	30 [mm]
	$i = 2,4$	0 [mm]
$\boldsymbol{I_P}$		$\begin{bmatrix} 4.5 & 0 & 0 \\ 0 & 2.6 & -0.01 \\ 0 & -0.01 & 2.6 \end{bmatrix} \times 10^{-2}$ [kg.m^2]
$\boldsymbol{m_{sad}}$	$i = 1, \ldots, 4$	1.2617 [kg]
$\boldsymbol{m_{li}}$	$i = 1,3,4$	0.495 [kg]
	$i = 2$	0.590 [kg]
$\boldsymbol{I_{li}}$	$i = 1,3,4$	diag (0.009;6.5;6.5)e-3 [kg.m^2]
	$i = 2$	diag (0.01;11.5;11.5)e-3 [kg.m^2]
$\boldsymbol{m_{con}}$	$i = 1,3$	0.1672 [kg]
$\boldsymbol{m_P}$		4.8041 [kg]
$\boldsymbol{b_i}$	$i = 1$	[-53;-98.5;-25] [mm]
	$i = 2$	[0;97.50;-4] [mm]
	$i = 3$	[53;-98.5;-25] [mm]
	$i = 4$	[0;127.5;-4] [mm]
$\boldsymbol{a_i}$	$i = 1$	[-185;-91;-42] [mm]
	$i = 2$	[29;-185;-42] [mm]
	$i = 3$	[243;-91;-42] [mm]
	$i = 4$	[29;243;-42] [mm]
$\boldsymbol{d_i}$	$i = 1$	180 [mm]
	$i = 2$	180 [mm]
	$i = 3$	180 [mm]
	$i = 4$	157.7 [mm]

REFERENCES

[1] Tsai, L., "Robot Analysis: The Mechanics of Serial and Parallel Manipulators", WILEY, 1999.

[2] Merlet, J. P., "Parallel Robots", Kluwer academic publishers, 2001.

[3] Wu, J., Yin, Z., "A Novel 4-DOF Parallel Manipulator H4", Parallel Manipulators, Towards New Applications, no. April, 2008, pp. 405–448.

[4] Altintas, Y., "Manufacturing Automation", London, UK: Cambridge University Press, 2000.

[5] Schmitz, T. L., Smith, K. S., "Machining Dynamics: Frequency Response to Improved Productivity", Springer US, 2009.

[6] Budak, E., "Analytical Models for High Performance Milling. Part I: Cutting Forces, Structural Deformations and Tolerance Integrity", Int. J. Mach. Tools Manuf., Vol. 46, No. 12–13, 2006, pp. 1478–1488.

[7] Budak, E., "Analytical Models for High Performance Milling. Part II: Process Dynamics and Stability", Int. J. Mach. Tools Manuf., Vol. 46, No. 12–13, 2006, pp. 1489–1499.

[8] Pedrammehr, S., Farrokhi, H., Rajab, A. K. S., Pakzad, S., Mahboubkhah, M., Ettefagh, M. M. and Sadeghi, M. H., "Modal Analysis of the Milling Machine Structure Through FEM and Experimental Test", Adv. Mat. Res., Vol. 383, 2012, pp. 6717-6721.

[9] Patwari, A. U., Faris, W. F., Nurul Amin, A. K. M., and Loh, S. K., "Dynamic Modal Analysis of Vertical Machining Centre Components", Adv. Acoust. Vib., Vol. 2009, pp. 1–10.

[10] Wu, Z., Xu, C., Zhang, J., Yu, D., and Feng, P., "Modal and Harmonic Response Analysis and Evaluation of Machine Tools", Proc. - 2010 Int. Conf. Digit. Manuf. Autom. ICDMA 2010, Vol. 1, 2010, pp. 929–933.

[11] Le Lan, J. V., Marty, A., and Debongnie, J. F., "A Stability Diagram Computation Method for Milling Adapted to Automotive Industry", CIRP - High Perform. Cut. 2006.

[12] Budak, E., Tunç, L. T., Alan, S., and Özgüven, H. N., "Prediction of Workpiece Dynamics and Its Effects on Chatter Stability in Milling", CIRP Ann. - Manuf. Technol., Vol. 61, No. 1, 2012, pp. 339–342.

[13] Mahdavinejad, R., "Finite Element Analysis of Machine and Workpiece Instability in Turning", Int. J. Mach. Tools Manuf., Vol. 45, No. 7–8, 2005, pp. 753–760.

[14] Doman, D. A., Warkentin, A., and Bauer, R., "Finite Element Modeling Approaches in Grinding", Int. J. Mach. Tools Manuf., Vol. 49, No. 2, 2009, pp. 109–116.

[15] Yuan, S. X., Wen, X. L., Zhang, Y. M., "Modal Analysis on the Truss Structures of Machine Tool", Adv. Mater. Res., Vol. 118–120, 2010, pp. 972–976.

[16] Sahu, S., Choudhury, B. B., and Biswal, B. B., "A Vibration Analysis of a 6 Axis Industrial Robot Using FEA", Mater. Today Proc., Vol. 4, No. 2, 2017, pp. 2403–2410.

[17] Zhang, X., Huang, R., Yao, S. and Dong, X., "Finite Element Analysis and Vibration Control of the Substation Charged Maintenance Robot", 4th International Conference on Applied Robotics for the Power Industry (CARPI), China, 2016, pp. 1–4.

[18] Flint, E., Anderson, E., "Multi-Degree of Freedom Parallel Actuation System Architectures for Motion Control", AIAA, No.4750, 2001, pp. 1–16.

[19] Mahboubkhah, M., Nategh, M., and Khadem, S., "A Comprehensive Study on the Free Vibration of Machine Tools' Hexapod Table", Int. J. Adv. Manuf. Technol., Vol. 40, No. 11–12, 2009, pp. 1239–1251.

[20] Mahboubkhah, M., Nategh, M., and Khadem, S., "Vibration Analysis of Machine Tool's Hexapod Table", Int. J. Adv. Manuf. Technol., Vol. 38, No. 11–12, 2008, pp. 1236–1243.

[21] Pedrammehr, S., Mahboubkhah, M., and Khani, N., "Natural Frequencies and Mode Shapes for Vibrations of Machine Tools' Hexapod Table", 1st Int. Conf. Acoust. Vib. (ISAV2011), Tehran, Iran, pp. 1–8.

[22] Pedrammehr, S., Mahboubkhah, M., Qazani, M. R. C., Rahmani, A., and Pakzad, S., "Forced Vibration Analysis of Milling Machine's Hexapod Table Under Machining Forces", Stroj. Vestnik/Journal Mech. Eng., Vol. 60, No. 3, 2014, pp. 158–171.

[23] Law, M., Ihlenfeldt, S., Wabner, M., Altintas, Y., and Neugebauer, R., "Position-Dependent Dynamics and Stability of Serial-Parallel Kinematic Machines", CIRP Ann. - Manuf. Technol., Vol. 62, No. 1, 2013, pp. 375–378.

[24] Sharifnia, M., Akbarzadeh, A., "Approximate Analytical Solution for Vibration of a 3-PRP Planar Parallel Robot with Flexible Moving Platform", Robotica, Vol. 34, No. 1, 2016, pp. 71–97.

[25] Pedrammehr, S., Danaei, B., Abdi, H., Masule, M. T. and Nahavandi, S., "Dynamic Analysis of Hexarot: Axis Symmetric Parallel Manipulator, Robotica", 2017, pp. 1-16. doi:10.1017/S0263574717000315.

[26] Zheng, K., Zhang, Q., "Comprehensive Analysis of the Position Error and Vibration Characteristics of Delta Robot", Adv. Robot., Vol. 30, No. 20, 2016, pp. 1322–1340.

[27] Chen, Z. S., Liu, M., Kong, M. X., and Ji, C., "Modal Analysis of High-Speed Parallel Manipulator with Flexible Links", Appl. Mech. Mater., Vol. 826, 2016, pp. 8–14.

[28] Guo, S., He, Y., Shi, L., Pan, S., and Tang, K., "Modal and Fatigue Analysis of Critical Components of an Amphibious Spherical Robot", Microsyst. Technol., Vol. 23, 2016, pp. 2233–2247.